Cell Reports, Volume *18*

Supplemental Information

BET-Bromodomain Inhibitors Engage the Host Immune System and Regulate Expression of the Immune Checkpoint Ligand PD-L1

Simon J. Hogg, Stephin J. Vervoort, Sumit Deswal, Christopher J. Ott, Jason Li, Leonie A. Cluse, Paul A. Beavis, Phillip K. Darcy, Benjamin P. Martin, Andrew Spencer, Anna K. Traunbauer, Irina Sadovnik, Karin Bauer, Peter Valent, James E. Bradner, Johannes Zuber, Jake Shortt, and Ricky W. Johnstone

SUPPLEMENTARY EXPERIMENTAL PROCEDURES

Retroviral transduction

Retroviral transduction of freshly isolated Eμ-*Myc* lymphomas with murine stem-cell virus-internal ribosomal entry site-green fluorescence protein (MSCV-IRES-GFP) and *Bcl2* (MSCV-IRES-GFP/Bcl-2) constructs were performed as previously described (Shortt et al., 2013). For *Myc* overexpression experiments, wild-type human *Myc* cDNA was subcloned into MSCV-IRES-GFP. For Pd-l1 rescue experiments, wild-type murine *Cd274* cDNA was subcloned into MSCV-IRES-BFP.

For inducible Myc knockdown experiments, shRNAs were expressed from the TRMPV-ns vector (27991, addgene) which has been previously described (Zuber et al., 2011). shRNAs targeting murine Myc (#1891 and #2105) or Renilla (REN) were subcloned into the TRMPV vector and transfected into HEK293T Phoenix packaging cells using standard calcium phosphate transfection protocols. Viral supernatant was used to transduce E μ-Myc lymphoma cells (#3) or AT3 cells in RetroNectin (TaKaRa, Shiga, Japan)-pre-coated 6-well plates (Becton Dickinson, Franklin Lakes, NJ). After 72 hours, GFP-positive cells were sorted by flow cytometry. To express an rtTA in the TRMPV-transduced cells, HEK293T cells were then transfected with the pRetroX-Tet-On Advanced vector using the same protocol. Viral supernatant was used to transduce the GFP-sorted TRMPV-transduced Eμ-Myc and AT3 cells which were then selected for 5 days using 1 mg/mL G418 (Invitrogen).

For inducible BRD4 knockdown, shRNAs targeting BRD4 were subcloned into the TRMPVIR Tet-shRNA expression vectors (27995, addgene) and transfected into HEK293T Phoenix packaging cells, as described above. The viral supernatant was used to transduce Eμ-Myc lymphoma cells (#1). After 72 hours, GFP-positive cells were sorted by flow cytometry and expanded in vitro. GFP-positive cells were treated in vitro with 1 μ g/mL doxycycline (DOX, Sigma-Aldrich) to induce shRNA/DsRed expression. Cell sorting was performed on a FACSAria Fusion flow sorter (BD Biosciences). The following shRNA sequences were used: Brd4 (#498), 5′-ACTATGTTTACAAATTGTT-3′, Brd4 (#500), 5′-AGCAGAACAAACCAAAGAA-3′, Myc (#1891) 5’-TGTTTCAACTGTTCTCGTCGT-3’, Myc (#2105) 3’-TACTATTTAAGTTTGAGGCAG-5’

Flow cytometry

Flow cytometry antibodies used in this study were: anti-mouse CD3 (pacific blue, 1:400, clone 17A2), anti-mouse CD4 (APC, 1:400, clone RM4-5), anti- anti-mouse CD8 (PE-Cy7, 1:400, clone 53-6.7), anti-mouse MHC class I (H-2Kb; Biotin, 1:200, clone AF6-88.5, anti-mouse PD-1 (FITC, 1:400, clone J43), anti-mouse Pd-l1 (PE, 1:100, clone MIH5), or anti-human PD-L1 (PE, 1:200, clone 29E.2A3. Biotinylated antibodies were subsequently incubated with Streptavidin-PE-Cy7 (1:1000, catalogue number 25-4317-82) or Streptavidin-Pacific Blue (1:1000, catalogue number 48-4317-82) for 30 minutes on ice. Anti-Armenian Hampster IgG (FITC, 1:400, catalogue number 554011), Mouse IgG2aκ (PE, 1:100, clone RTK2758), Mouse IgG2bκ (PE, 1:200, catalogue number 559529), and Mouse IgG2aκ (Biotin, 1:200, clone eBM2a) were used as isotype control antibodies, respectively. All antibodies were purchased from BioLegend (San Diego, CA), eBiosciences (San Diego, CA), or BD Bioscience (San Diego, CA)

Quantatative real-time PCR

qRT-PCR primer sequences were:
Mus musculus Cd274 F:TTCGTACGGGCGTTTACTATC
R:TCCCGTTCTACAGGGAATCT,
Mus musculus Gapdh F:CCTTCATTGACCTCAACTAC
R:GGAAGGCCATGCCAGTGAGC,
Mus musculus Actin F:AGCTTCTTTGCAGCTCCTTCGTTG
R:TTCTGACCCATTCCCACCATCACA,
Mus musculus endogenous *Myc* F:CAGCTCCTCCTCGAGTTAG
R:TGAGGAAACGACGAGAACAG, *Mus musculus* transgenic *Myc*
F:TCGAACAGCTTCGAAACTCTGGTG R: TTAAATCGAAGTGGACTGCTGGCG,
Homo sapiens MYC F: GGACGACGAGACCTTCATCAA R:
CCAGCTTCTCTGAGACGAGCTT,
Homo sapiens CD274 F: TATGGTGGTGCCGACTACAA
R:TGGCTCCCAGAATTACCAAG,
Homo sapiens L32 F: TTCCTGGTCCACAATGTCAAG R: TTGTGAGCGATCTCGGCAC

4-thiouridine (4sU) labeling of newly transcribed RNA

Cell pellets were collected and total RNA was collected using TRIzol (Thermo Fisher). 4sU-labelled RNA was then biotinylated with 2µg EZ-link biotin-HPDP (Pierce) per µg of RNA in biotinylation buffer for 1.5 hours at room temperature. The biotinylated RNA was extracted using an equal volume of chloroform, precipitated in ethanol, and resuspended in water. The biotinylated RNA fraction was then purified using µMacs Streptavidin kit (Miltenyi) and washed three times with washing buffer (5mM Tris-HCl [pH7.5], 0.5mM EDTA, 1mM NaCl in H2O). The biotinylated RNA was eluted from the magnetic beads using 100mM DTT and purified using the RNeasy MinElute cleanup kit (Qiagen). cDNA was synthesized according to the manufacturers instructions (Promega, Sydney, NSW) and quantitative PCR analysis of samples was performed on the 7900HT Fast Real-Time PCR System (Applied Biosystems, Mulgrave, VIC, Australia) with SYBR-green ROX mix (Agilent, Mulgrave, VIC, Australia).

RNA sequencing and analysis

Early passage Eµ-Myc lymphoma #1 variants (#1.1 and #1.2) were cultured in the presence or absence of 250nM JQ1 for 2 hours in duplicate and cell pellets collected. Total RNA was extracted using the Nucleospin® RNA extraction kit (Macherey-Nagel, Bethlehem, PA) as per the manufacturer's instructions. cDNA libraries were prepared and then processed for using TruSeq RNA library Prep Kit (Illumina, San Diego, CA, USA) and paired-end RNA-sequencing was performed on the HiSeq 2000. Short-read data was processed using Seqliner RNA-seq pipeline (seqliner.org). Sample QC was first performed and overrepresented sequences identified using FastQC (Babraham Bioinformatics, Babraham Institute). The RNA sequencing reads were trimmed using cutadapt(v1.7) (Martin, 2011) to remove poor quality ends. Read data was then aligned using TopHat/bowtie2 (Kim et al., 2013) to the mouse reference genome (GRCm38/mm10). Read counting was performed with HTSeq-Count from HTSeq (Anders S, 2014) using transcript annotation from Ensembl Release 73 (Flicek et al., 2014). The Voom-LIMMA workflow (Law et al., 2014) was used to normalise data and compute statistical significance of differential gene expression. GSEA2-2.2.2 was used for identification of enriched signatures obtained from the MSigDB Hallmarks datasets (Liberzon et al., 2015).

Chromatin Immunoprecipitation library preparation and sequencing analysis

DNA was quantified using Qubit dsDNA HS Assay Kit (Thermo Fisher Scientific) and indexed libraries were prepared using KAPA Hyper Prep Kit for Illumina platforms (Kapa Biosystems) and the SeqCap Adapter Kit (Roche) following vendor's instructions. For library preparation of DNA immunoprecipitated with an anti-Myc antibody, libraries were prepared with the Nugen Ovation Ultralow system (v2, using Nugen protocol M01379v3). Library quality and quantity was evaluated with a Bioanalyser D1000 chip (Agilent Technologies) and size selected between 200bp and 500bp using a Pippin Prep System (Sage Science). Final QC was done using a Tape Station High Sensitivity DNA Analysis Kit (Agilent Technologies). For sequencing analysis of immunoprecipitated DNA with anti-Myc antibody, libraries were then pooled and sequenced on a HiSeq1500 (Illumina) and 13 to 18 million single-end 50 bp reads were generated per sample. For sequencing analysis of DNA immunoprecipitated with anti-BRD4 and RNA Polymerase II antibodies, libraries were then pooled and sequenced on a HiSeq2500 (Illumina) and 13 to 18 million single-end 50 bp reads were generated per sample. CASAVA (v1.8.2) was used for demultiplexing. The Fastq files generated by sequencing were aligned to the mouse reference genome (GRCm38/mm10) using bowtie (v2.2.3). Samtools (v1.3) was used for manipulation of SAM and BAM files, after which MACS (v2.0.10) was used for peak calling. Browser viewable TDF files were generated using IGVTools (v2.3.72) and ChIP-Seq tracks were visualized using IGV (v2.3.55). HOMER (v4.8.3) was used for quantification and annotation of the ChIP-Seq datasets after which R was used for visualization.

QuantSeq 3'-mRNA library preparation, sequencing and analysis

3'-mRNA sequencing reads were demultiplexed using CASAVAv1.8.2 and low-quality reads Q<30 were removed. The RNA sequencing reads were trimmed at the 5'end using cutadapt(v1.9)(Martin, 2011) to remove bias introduced by random primers used in the library preparation and 3'end trimming was performed to eliminate poly-A-tail derived reads. Reads were mapped to the reference genomes (hg19 for human and mm10 for mouse) using HISAT2. Read counting was performed using featureCounts part of the subread v1.5.0 software package (Liao et al., 2014). Differential gene expression analysis was performed using Voom-LIMMA. R was used for general figure preparation and HOMER was used for metagene analysis.

Generation and analyses of a PDAC mouse model harboring Tet-repressible (Tet-off) Myc

Tet-off Myc murine pancreatic cancer cells were generated and characterized as previously described (Lito et al., 2014). In brief, pancreatic progenitor cells isolated from a murine fetus (ED17.5–18.5) harboring a conditional endogenous KrasG12D allele (lox-STOP-lox-KrasG12D) (Jackson et al., 2001) and a conditional Trp53 deletion (Trp53-fl/fl) (Jonkers et al., 2001) were co-transduced with two retroviral constructs (pSIN-TRE3G-Myc-IRES-GFP and MSCV-Luc2-PGK-CreERT2-IRES-tTA; cloning details available upon request). After 4 days of 4-hydroxy-tamoxifen treatment, cells were orthotopically injected into the pancreas of syngeneic recipient mice, which were monitored using bioluminescence imaging (Caliper Life Sciences). Emerging tumors were characterized to display histological features of human pancreatic ductal adenocarcinoma (PDAC) and used to derive a cell line, which was cultured in DMEM (Gibco-Invitrogen) with 10% FBS, 20mM glutamate, 10mM sodium pyruvate, 100U/ml penicillin and 100 µg/ml streptomycin. For Pd-l1 expression studies, cells were treated with 250 nM JQ1, 1 µg/ml Doxycycline (D9891, Sigma Aldrich) and/or 50 ng/ml mouse recombinant IFN-γ (14-8311-63, Affymetrix) in various combinations / time courses. For flow cytometry analysis, cells were incubated with mouse TruStain fcX Fc receptor blocking agent (Biolegend) for 15 min at room temperature, stained with PE-conjugated anti-mouse Cd274 (124307, BioLegend) diluted 1:400 in FACS buffer (10% FCS in PBS), washed twice using FACS buffer, and analyzed on an LSR Fortessa (BD) flow cytometer. Data analysis was performed using FlowJo software (Treestar). For immunoblotting of Myc, about 20 µg of whole-cell lysate (RIPA lysis buffer + 1x protease inhibitor cocktail, 4693159001, Roche Diagnostics) were loaded onto each lane (NuPAGE Novex 4-12% Bis-Tris Gels, NP0322BOX, Life Technologies). Protein extracts were resolved by SDS polyacrylamide gel electrophoresis (SDS–PAGE) and transferred to PVDF membrane (Thermo Fisher Scientific) for blotting (70 V, 90 min). The antibodies used for WB were: Myc (56058, Cell Signaling), β-actin (A3854, Sigma-Aldrich) and secondary antibody anti-rabbit IgG, HRP-linked (7074, Cell Signaling).

Hi-C

Bedtools2.21 was used to identify Brd4 peaks interacting with 3D chromatin-loops identified in CH12-LX mouse B-lymphoblasts using HiCCUPS (GSE63525). The Hi-C contact map and indicated histone marks for the genomic locus encompassing Cd274 was visualized using Juicebox software (Durand et al., 2016; Rao et al., 2014).

Immunoblot

Cell lysate preparation, SDS polyacrylamide gel electrophoresis and immunoblotting were performed according to standard protocols (Shortt et al., 2013) with the following primary antibodies: anti-Brd4 (Abcam), anti-phospho-STAT1 [Tyr701] (Cell Signalling Technologies), anti-STAT1 (BD Biosciences), and α-tubulin (Merck KGaA, Darmstadt, Germany).

Supplementary References

Durand, N.C., Robinson, J.T., Shamim, M.S., Machol, I., Mesirov, J.P., Lander, E.S., and Aiden, E.L. (2016). Juicebox Provides a Visualization System for Hi-C Contact Maps with Unlimited Zoom. Cell systems 3, 99-101.

Flicek, P., Amode, M.R., Barrell, D., Beal, K., Billis, K., Brent, S., Carvalho-Silva, D., Clapham, P., Coates, G., Fitzgerald, S., et al. (2014). Ensembl 2014. Nucleic Acids Res 42, D749-755.

Jackson, E.L., Willis, N., Mercer, K., Bronson, R.T., Crowley, D., Montoya, R., Jacks, T., and Tuveson, D.A. (2001). Analysis of lung tumor initiation and progression using conditional expression of oncogenic K-ras. Genes Dev 15, 3243-3248.

Jonkers, J., Meuwissen, R., van der Gulden, H., Peterse, H., van der Valk, M., and Berns, A. (2001). Synergistic tumor suppressor activity of BRCA2 and p53 in a conditional mouse model for breast cancer. Nat Genet 29, 418-425.

Kim, D., Pertea, G., Trapnell, C., Pimentel, H., Kelley, R., and Salzberg, S.L. (2013). TopHat2: accurate alignment of transcriptomes in the presence of insertions, deletions and gene fusions. Genome Biol 14, R36.

Kress, T.R., Pellanda, P., Pellegrinet, L., Bianchi, V., Nicoli, P., Doni, M., Recordati, C., Bianchi, S., Rotta, L., Capra, T., et al. (2016). Identification of MYC-Dependent Transcriptional Programs in Oncogene-Addicted Liver Tumors. Cancer Res 76, 3463-3472.

Law, C.W., Chen, Y., Shi, W., and Smyth, G.K. (2014). voom: Precision weights unlock linear model analysis tools for RNA-seq read counts. Genome Biol 15, R29.

Liao, Y., Smyth, G.K., and Shi, W. (2014). featureCounts: an efficient general purpose program for assigning sequence reads to genomic features. Bioinformatics 30, 923-930.
Liberzon, A., Birger, C., Thorvaldsdottir, H., Ghandi, M., Mesirov, J.P., and Tamayo, P. (2015). The Molecular Signatures Database (MSigDB) hallmark gene set collection. Cell systems 1, 417-425.
Lito, P., Saborowski, A., Yue, J., Solomon, M., Joseph, E., Gadal, S., Saborowski, M., Kastenhuber, E., Fellmann, C., Ohara, K., et al. (2014). Disruption of CRAF-mediated MEK activation is required for effective MEK inhibition in KRAS mutant tumors. Cancer Cell 25, 697-710.
Martin, M.B. (2011). Cutadapt removes adapter sequences from high-throughput sequencing reads. EMBnet 17, 10-12.
Rao, S.S., Huntley, M.H., Durand, N.C., Stamenova, E.K., Bochkov, I.D., Robinson, J.T., Sanborn, A.L., Machol, I., Omer, A.D., Lander, E.S., et al. (2014). A 3D map of the human genome at kilobase resolution reveals principles of chromatin looping. Cell 159, 1665-1680.
Shortt, J., Martin, B.P., Newbold, A., Hannan, K.M., Devlin, J.R., Baker, A.J., Ralli, R., Cullinane, C., Schmitt, C.A., Reimann, M., et al. (2013). Combined inhibition of PI3K-related DNA damage response kinases and mTORC1 induces apoptosis in MYC-driven B-cell lymphomas. Blood 121, 2964-2974.
Tasdemir, N., Banito, A., Roe, J.S., Alonso-Curbelo, D., Camiolo, M., Tschaharganeh, D.F., Huang, C.H., Aksoy, O., Bolden, J.E., Chen, C.C., et al. (2016). BRD4 Connects Enhancer Remodeling to Senescence Immune Surveillance. Cancer discovery 6, 612-629.
Zuber, J., Shi, J., Wang, E., Rappaport, A.R., Herrmann, H., Sison, E.A., Magoon, D., Qi, J., Blatt, K., Wunderlich, M., et al. (2011). RNAi screen identifies Brd4 as a therapeutic target in acute myeloid leukaemia. Nature 478, 524-528.

SUPPLEMENTARY FIGURES

(A)

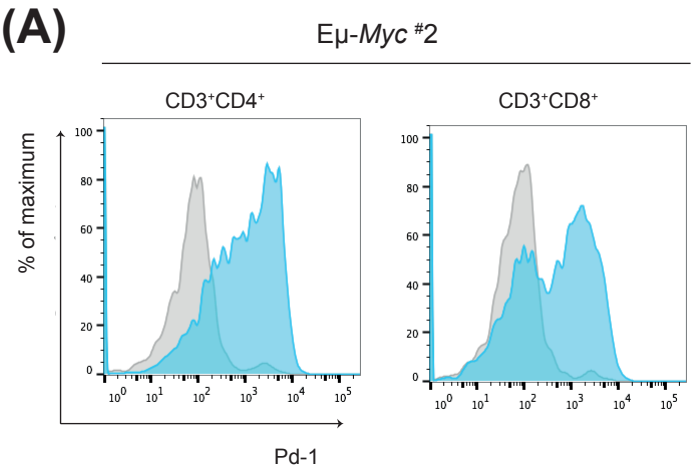

(B)

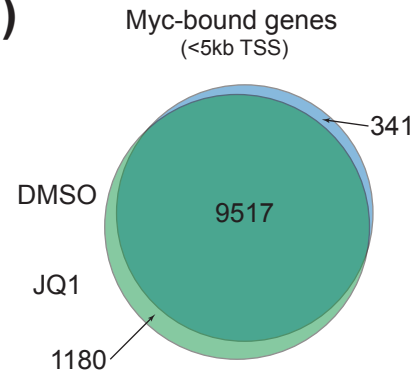

(C)

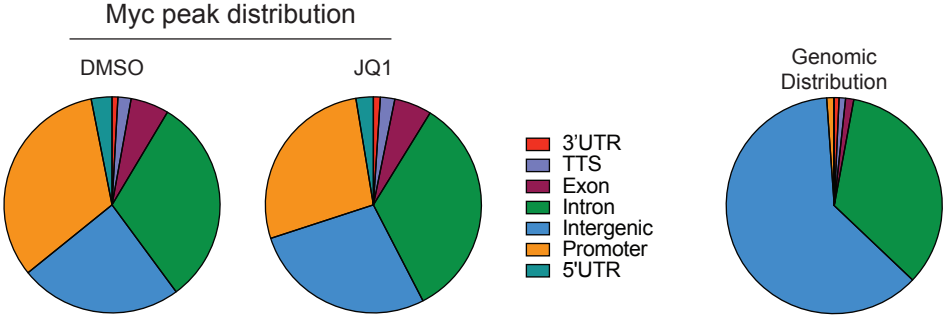

(D)

MYC ChIP-seq; DMSO-treated

Transcription Factor	Motif	Log P-value	Rank
c-Myc		-4.742e3	1
Elk1		-1.08e3	3
KLF5		-4.93e2	4

MYC ChIP-seq; JQ1-treated

Transcription Factor	Motif	Log P-value	Rank
c-Myc		-6.134e3	1
Fli1		-1.317e3	3
NRF		-9.561e2	4

(E)

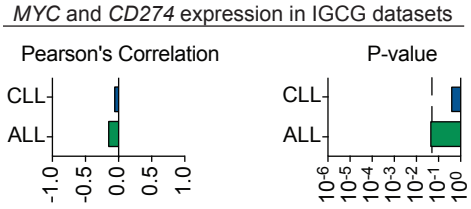

Figure S1, related to figure 1 and 3. Tumor-infiltrating lymphocytes express Pd-1 **(A)** Spleens from C57BL/6 mice bearing Eμ-Myc lymphomas were harvested and stained by FACS for cell surface Cd3, Cd4 and Cd8. Expression of Pd-1 is shown using an anti-Pd1 Ab (blue histogram) with isotype control staining shown in grey histograms. Analysis of Myc ChIP-seq datasets in Eμ-*Myc* cells; **(B)** Venn-diagram representing the number of Myc-bound genes (within 5kb of the TSS) in DMSO and JQ1 treated conditions. **(C)** Genomic distribution of Myc peaks across annotated regions of the genome in DMSO and JQ1 treated conditions. The contribution of annotated regions is presented in the bottom panel. **(D)** De novo motif discovery on Myc bound sites in DMSO and JQ1 treated conditions. **(E)** Correlation of *MYC* and *CD274* expression was measured in publically available datasets from the International Cancer Genomics Consortium (IGCG) using Pearson's correlation coefficient.

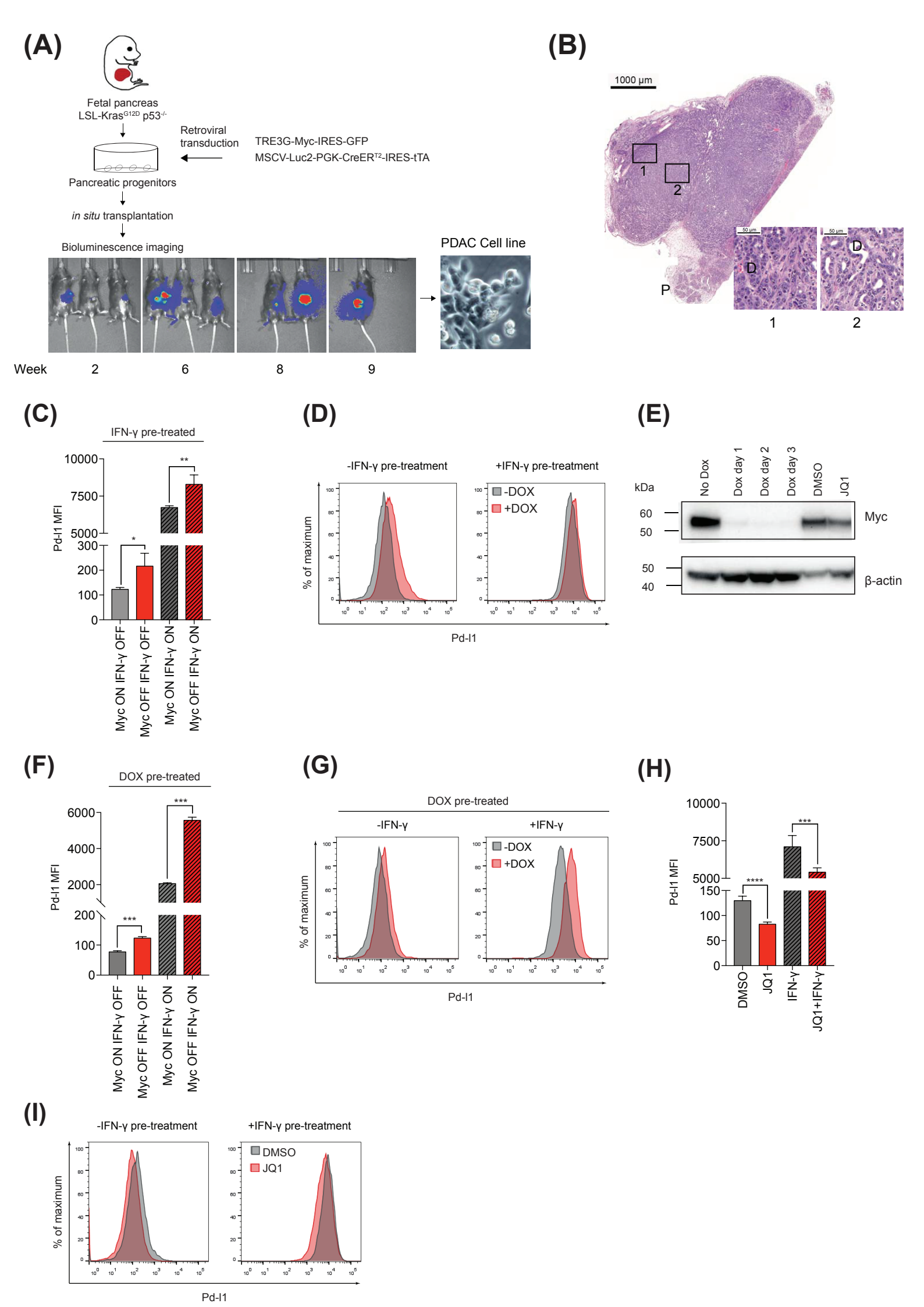
(A)
Fetal pancreas
LSL-Kras^{G12D} p53$^{-/-}$
Retroviral transduction
TRE3G-Myc-IRES-GFP
MSCV-Luc2-PGK-CreER^{T2}-IRES-tTA
Pancreatic progenitors
in situ transplantation
Bioluminescence imaging
PDAC Cell line
Week 2 6 8 9
(B)
1000 μm
1
2
P
D
D
50 μm
1
2
(C)
IFN-γ pre-treated
Pd-l1 MFI
10000
7500
5000
300
200
100
0
*
**
Myc ON IFN-γ OFF
Myc OFF IFN-γ OFF
Myc ON IFN-γ ON
Myc OFF IFN-γ ON
(D)
-IFN-γ pre-treatment
+IFN-γ pre-treatment
-DOX
+DOX
% of maximum
Pd-l1
(E)
kDa
No Dox
Dox day 1
Dox day 2
Dox day 3
DMSO
JQ1
60
50
Myc
50
40
β-actin
(F)
DOX pre-treated
Pd-l1 MFI
6000
4000
2000
200
100
0
***
***
Myc ON IFN-γ OFF
Myc OFF IFN-γ OFF
Myc ON IFN-γ ON
Myc OFF IFN-γ ON
(G)
DOX pre-treated
-IFN-γ
+IFN-γ
-DOX
+DOX
% of maximum
Pd-l1
(H)
Pd-l1 MFI
10000
7500
5000
150
100
50
0
****
***
DMSO
JQ1
IFN-γ
JQ1+IFN-γ
(I)
-IFN-γ pre-treatment
+IFN-γ pre-treatment
DMSO
JQ1
% of maximum
Pd-l1

Figure S2, related to figure 3. Development and characterization of tet-OFF Myc PDAC mouse model. **(A)** Schematic and in vivo imaging data for the tet-OFF Myc mouse model. Pancreatic progenitor cells from E17.5-E18.5 embryos from LSL-Kras^{G12D}; p53fl/fl mice were harvested and retrovirally transduced with the indicated plasmids after two days of culture. After 4 days of 4-hydroxy-tamoxifen treatment, cells were in situ transplanted into C57BL/6 mice and assessed for luciferase expression using in vivo imaging system. Tumor cells were harvested and cultured in normal DMEM medium containing fetal bovine serum. **(B)** H&E staining shows intermediate to high grade pancreatic ductal adenocarcinoma with less conspicuous (1) and well differentiated ductal structures (2). D = ductal differentiation, P = remnants of pre-existent pancreatic parenchyma (including islets). Genetic depletion of *Myc* does not affect Pd-l1 expression; (**C, D)** PDAC cells expressing dox-inducible Myc were either pre-treated with 50 ng/mL IFN-γ (for 24 hr) or left untreated, followed by treatment with Dox or DMSO for 48 hr. Cell surface expression of Pd-l1 was assessed by FACS. MFI (mean ± SD from 4 experiments) is shown. **(E)** Western blot analysis for expression of Myc and β-actin was performed using lysates from PDAC cells cultured in the presence and absence of Dox for 24 and 48 hr. **(F, G)**. PDAC cells expressing dox-inducible Myc were either pre-treated with Dox for 24 hr or left untreated before 50 ng/mL IFN-γ or vehicle treatment for 48 hr (for Dox pre-treated samples, Dox treatment was continued during these 48 h). **(H, I)** PDAC cells expressing dox-inducible Myc were either pre-treated with 50 ng/mL IFN-γ (for 24 hr) or left untreated, followed by treatment with 250 nM JQ1 or DMSO for 48 hr. Cell surface expression of Pd-l1 was assessed by FACs. MFI (mean ± SD from 4 experiments) is shown.

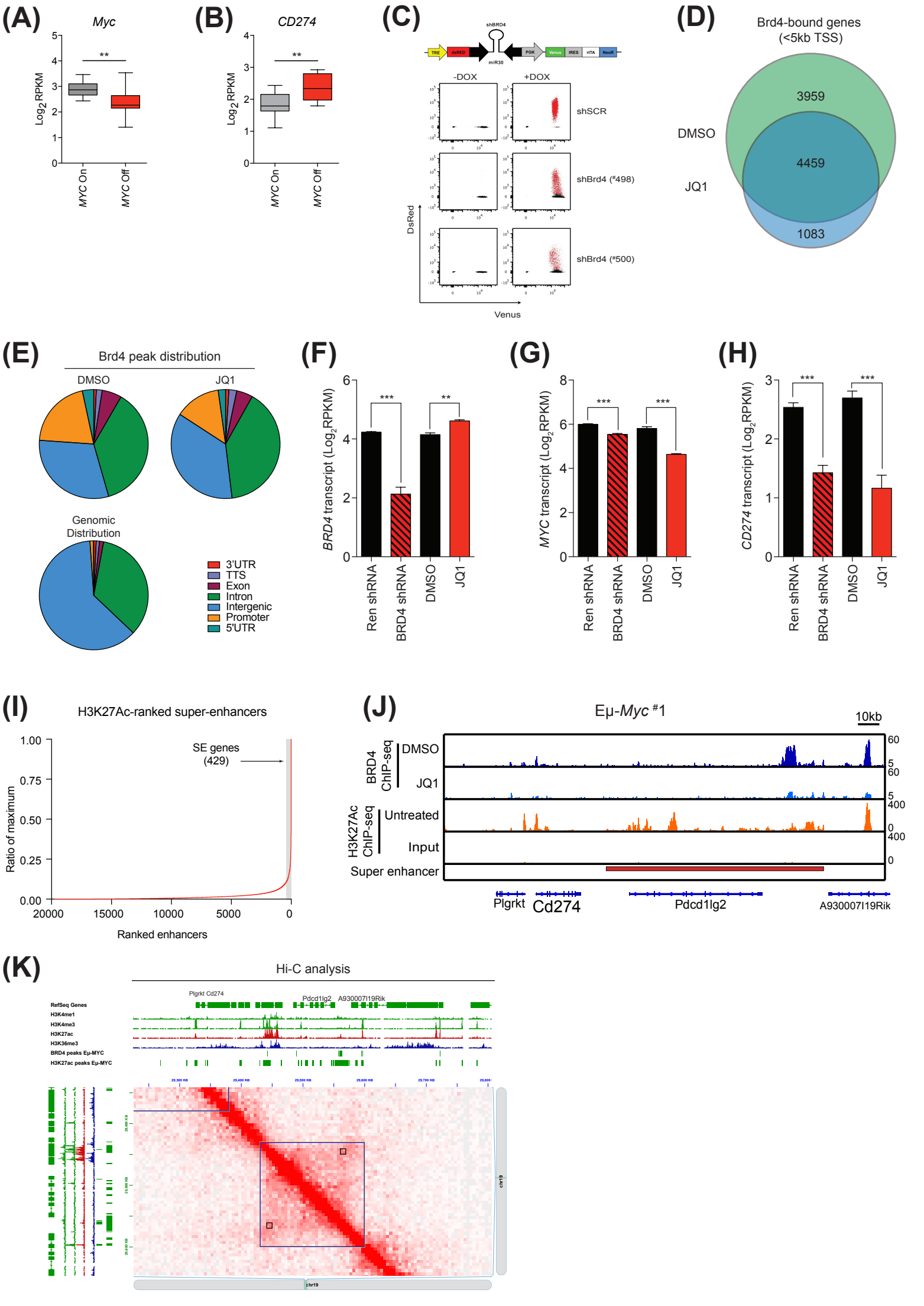
(A)
Myc
Log2 RPKM
MYC On
MYC Off
(B)
CD274
Log2 RPKM
MYC On
MYC Off
(C)
shBRD4
TRE
dsRED
miR30
PGK
Venus
IRES
rtTA
NeoR
-DOX
+DOX
shSCR
shBrd4 (#498)
shBrd4 (#500)
DsRed
Venus
(D)
Brd4-bound genes
(<5kb TSS)
DMSO
JQ1
3959
4459
1083
(E)
Brd4 peak distribution
DMSO
JQ1
Genomic
Distribution
3'UTR
TTS
Exon
Intron
Intergenic
Promoter
5'UTR
(F)
BRD4 transcript (Log2RPKM)
Ren shRNA
BRD4 shRNA
DMSO
JQ1
(G)
MYC transcript (Log2RPKM)
Ren shRNA
BRD4 shRNA
DMSO
JQ1
(H)
CD274 transcript (Log2RPKM)
Ren shRNA
BRD4 shRNA
DMSO
JQ1
(I)
H3K27Ac-ranked super-enhancers
SE genes
(429)
Ratio of maximum
Ranked enhancers
(J)
Eμ-Myc #1
10kb
BRD4
ChIP-seq
DMSO
JQ1
H3K27Ac
ChIP-seq
Untreated
Input
Super enhancer
Plgrkt
Cd274
Pdcd1lg2
A930007I19Rik
(K)
Hi-C analysis
Plgrkt Cd274
Pdcd1lg2
A930007I19Rik
RefSeq Genes
H3K4me1
H3K4me3
H3K27ac
H3K36me3
BRD4 peaks Eμ-MYC
H3K27ac peaks Eμ-MYC

Figure S3, related to figure 3 and 4. Reanalysis of RNA-seq data (GSE76062) from Kress and colleagues (Kress et al., 2016). Data from a tet-MYC off model of liver carcinoma demonstrating that upon *MYC* inactivation, *CD274* mRNA is significantly upregulated. Data represents log_2RPKM values for **(A)** *MYC* and **(B)** *CD274* expression in *MYC* On (n=16) and *MYC* Off (n=8) samples (**p<0.01, Student's t test). Genetic depletion of *Brd4* downregulates Pd-l1 expression in Eμ-*Myc* lymphoma; **(C)** Eμ-*Myc* lymphoma #1 were transduced with TRMPVIR.shScrambled, TRMPVIR.shBRD4.498, and TRMPVIR.shBRD4.500 and exposed to doxycycline (DOX) to induce the DsRed-shRNA gene cassette. Representative flow cytometry plots show induction of DsRed following DOX treatment for each construct. **(D)** Venn-diagram representing the number of genes bound Brd4 (within 5kb of the TSS) in DMSO and JQ1 treated conditions. **(E)** Genomic distribution of Brd4 peaks across annotated regions of the genome in DMSO and JQ1 treated conditions. The contribution of annotated regions is presented in the bottom panel. Reanalysis of RNA-seq data (GSE74324) from Tasemir and colleagues; Studies using IMR90 $Hras^{V12}$-transformed human fibroblasts (Tasdemir et al., 2016) cells demonstrate that *CD274* is consistently downregulated following genetic depletion of *BRD4* or JQ1 treatment in the absence of substantive downregulation of *MYC*. Data represents log_2RPKM values for **(F)** *BRD4* **(G)** *MYC* and **(H)** *CD274* expression (**p<0.01, ***p<0.001, Student's t test). Identification of super-enhancers and 3D chromatin interactions in Eμ-*Myc* lymphoma; **(I)** Identification of super-enhancers in Eμ-*Myc* cells based on H3K27Ac ChIP-Seq data obtained from public dataset (GSE51004). Stitched enhancers (12.5kb distance) were ranked by H3K27Ac signal and normalized to the maximum, resulting in the identification of 429 super-enhancers. **(J)** H3K27Ac and Brd4 occupancy tracks and super-enhancer peak track across the extended *Cd274* genomic locus. **(K)** Visualization of Hi-C data obtained from CH12-LX mouse B-lymphoblasts (GSE63525) and corresponding H3K4Me3, H3K4Me1, H3K27Ac and H3K36Me3 ChIP-seq data, with Brd4 and H3K27Ac peaks identified in Eμ-*Myc* indicated underneath. The blue box indicates identified chromatin loops with contact domains indicated by black boxes.

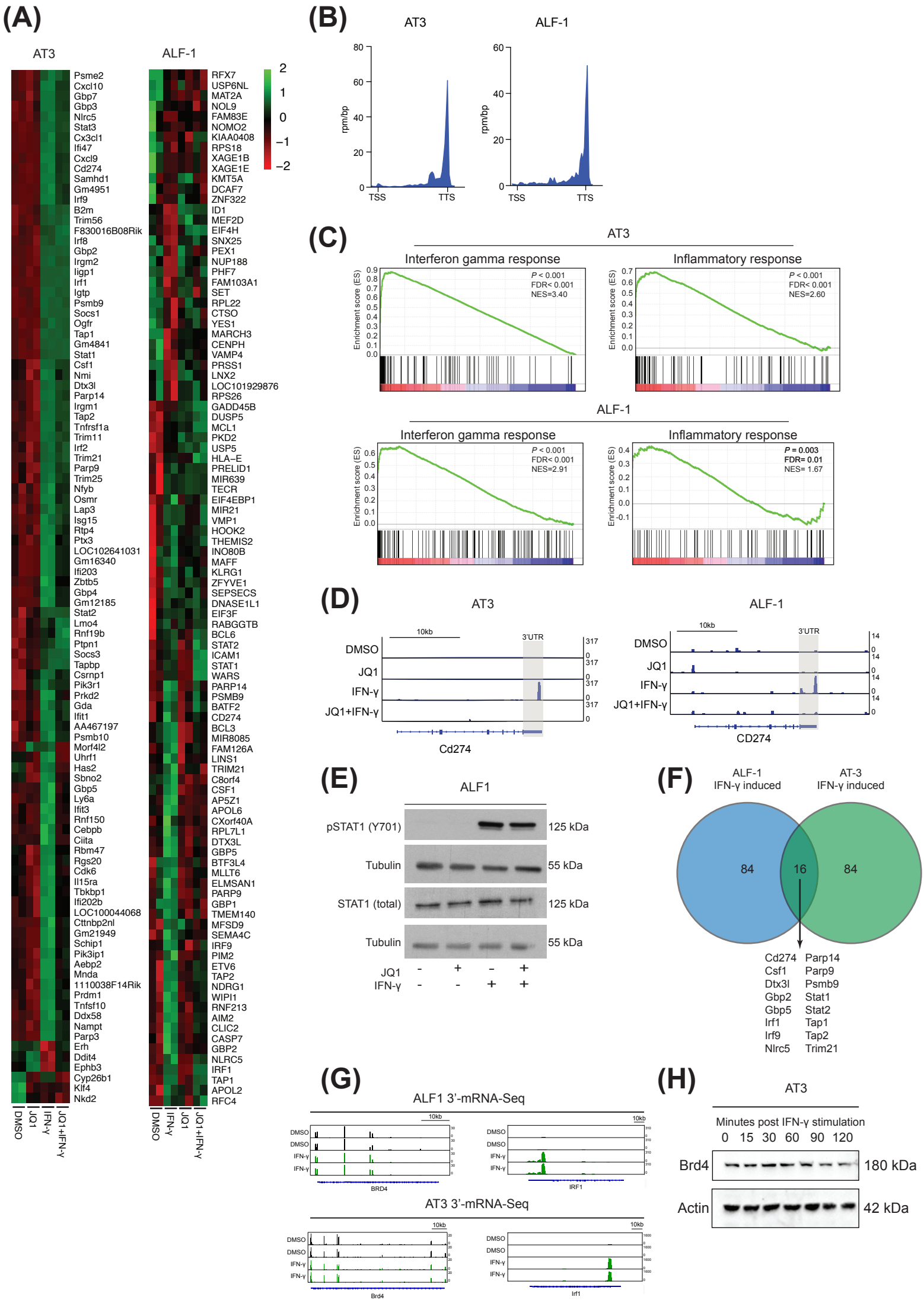
(A)
AT3
ALF-1
Psme2
Cxcl10
Gbp7
Gbp3
Nlrc5
Stat3
Cx3cl1
Ifi47
Cxcl9
Cd274
Samhd1
Gm4951
Irf9
B2m
Trim56
F830016B08Rik
Irf8
Gbp2
Irgm2
Iigp1
Irf1
Igtp
Psmb9
Socs1
Ogfr
Tap1
Gm4841
Stat1
Csf1
Nmi
Dtx3l
Parp14
Irgm1
Tap2
Tnfrsf1a
Trim11
Irf2
Trim21
Parp9
Trim25
Nfyb
Osmr
Lap3
Isg15
Rtp4
Ptx3
LOC102641031
Gm16340
Ifi203
Zbtb5
Gbp4
Gm12185
Stat2
Lmo4
Rnf19b
Ptpn1
Socs3
Tapbp
Csrnp1
Pik3r1
Prkd2
Gda
Ifit1
AA467197
Psmb10
Morf4l2
Uhrf1
Has2
Sbno2
Gbp5
Ly6a
Ifit3
Rnf150
Cebpb
Ciita
Rbm47
Rgs20
Cdk6
Il15ra
Tbkbp1
Ifi202b
LOC100044068
Cttnbp2nl
Gm21949
Schip1
Pik3ip1
Aebp2
Mnda
1110038F14Rik
Prdm1
Tnfsf10
Ddx58
Nampt
Parp3
Erh
Ddit4
Ephb3
Cyp26b1
Klf4
Nkd2
RFX7
USP6NL
MAT2A
NOL9
FAM83E
NOMO2
KIAA0408
RPS18
XAGE1B
XAGE1E
KMT5A
DCAF7
ZNF322
ID1
MEF2D
EIF4H
SNX25
PEX1
NUP188
PHF7
FAM103A1
SET
RPL22
CTSO
YES1
MARCH3
CENPH
VAMP4
PRSS1
LNX2
LOC101929876
RPS26
GADD45B
DUSP5
MCL1
PKD2
USP5
HLA–E
PRELID1
MIR639
TECR
EIF4EBP1
MIR21
VMP1
HOOK2
THEMIS2
INO80B
MAFF
KLRG1
ZFYVE1
SEPSECS
DNASE1L1
EIF3F
RABGGTB
BCL6
STAT2
ICAM1
STAT1
WARS
PARP14
PSMB9
BATF2
CD274
BCL3
MIR8085
FAM126A
LINS1
TRIM21
C8orf4
CSF1
AP5Z1
APOL6
CXorf40A
RPL7L1
DTX3L
GBP5
BTF3L4
MLLT6
ELMSAN1
PARP9
GBP1
TMEM140
MFSD9
SEMA4C
IRF9
PIM2
ETV6
TAP2
NDRG1
WIPI1
RNF213
AIM2
CLIC2
CASP7
GBP2
NLRC5
IRF1
TAP1
APOL2
RFC4
2
1
0
−1
−2
DMSO
JQ1
IFN-γ
JQ1+IFN-γ
(B)
AT3
ALF-1
rpm/bp
TSS
TTS
(C)
AT3
Interferon gamma response
Inflammatory response
Enrichment score (ES)
P < 0.001
FDR< 0.001
NES=3.40
NES=2.60
ALF-1
P < 0.001
FDR< 0.001
NES=2.91
P = 0.003
FDR= 0.01
NES= 1.67
(D)
AT3
ALF-1
10kb
3'UTR
DMSO
JQ1
IFN-γ
JQ1+IFN-γ
Cd274
(E)
ALF1
pSTAT1 (Y701)
125 kDa
Tubulin
55 kDa
STAT1 (total)
125 kDa
Tubulin
55 kDa
JQ1
IFN-γ
(F)
ALF-1
IFN-γ induced
AT-3
IFN-γ induced
84
16
84
Cd274
Csf1
Dtx3l
Gbp2
Gbp5
Irf1
Irf9
Nlrc5
Parp14
Parp9
Psmb9
Stat1
Stat2
Tap1
Tap2
Trim21
(G)
ALF1 3'-mRNA-Seq
BRD4
IRF1
AT3 3'-mRNA-Seq
Brd4
Irf1
(H)
AT3
Minutes post IFN-γ stimulation
0 15 30 60 90 120
Brd4
180 kDa
Actin
42 kDa

Figure S4, related to figure 5. JQ1 treatment suppresses IFN-γ-induced Pd-l1 expression in a murine mammary tumour cell line (AT3) and a patient-derived plasma cell leukaemia cell line (ALF-1). **(A)** Gene expression heatmap shows the top 100 IFN-γ-regulated genes by 3'-mRNA-Seq analysis of AT3 or ALF-1 cells treated for 2 hours in the presence of 1μM JQ1, 1ng/mL IFN-γ, combination of JQ1 and IFN-γ, or DMSO vehicle. Row-normalized values are represented. **(B)** Metagene analysis of strand specific 3'-mRNA-Seq reads indicating accurate mapping to the 3'UTR **(C)** GSEA enrichment score plots show significant correlation between genes induced by IFN-γ and interferon gamma and inflammatory response signatures. **(D)** Representative image of 3'-mRNA-Seq reads mapped to the *CD274* locus across treatment conditions. **(E)** AT3 cells were treated as in (A) prior to assessment of phospho-STAT1 (Y701) and total-STAT1 by immunoblot. Tubulin was used as the loading control. **(F)** Venn diagram representing the overlap between IFN-γ-induced genes in AT3 and ALF1 cells identified a common subset of 16 overlapping genes.IFN-γ does not increase BRD4 expression; **(G)** 3'-mRNA-Seq reads mapped to the Brd4 and Irf1 loci in ALF-1 and AT3 cells cultured in the presence or absence of 1ng/mL IFN-γ. **(H)** AT3 cells were treated with a dose titration of recombinant mouse IFN-γ (1ng/mL) prior to assessment of Brd4 protein levels by immunoblot. Actin was used as the loading control.

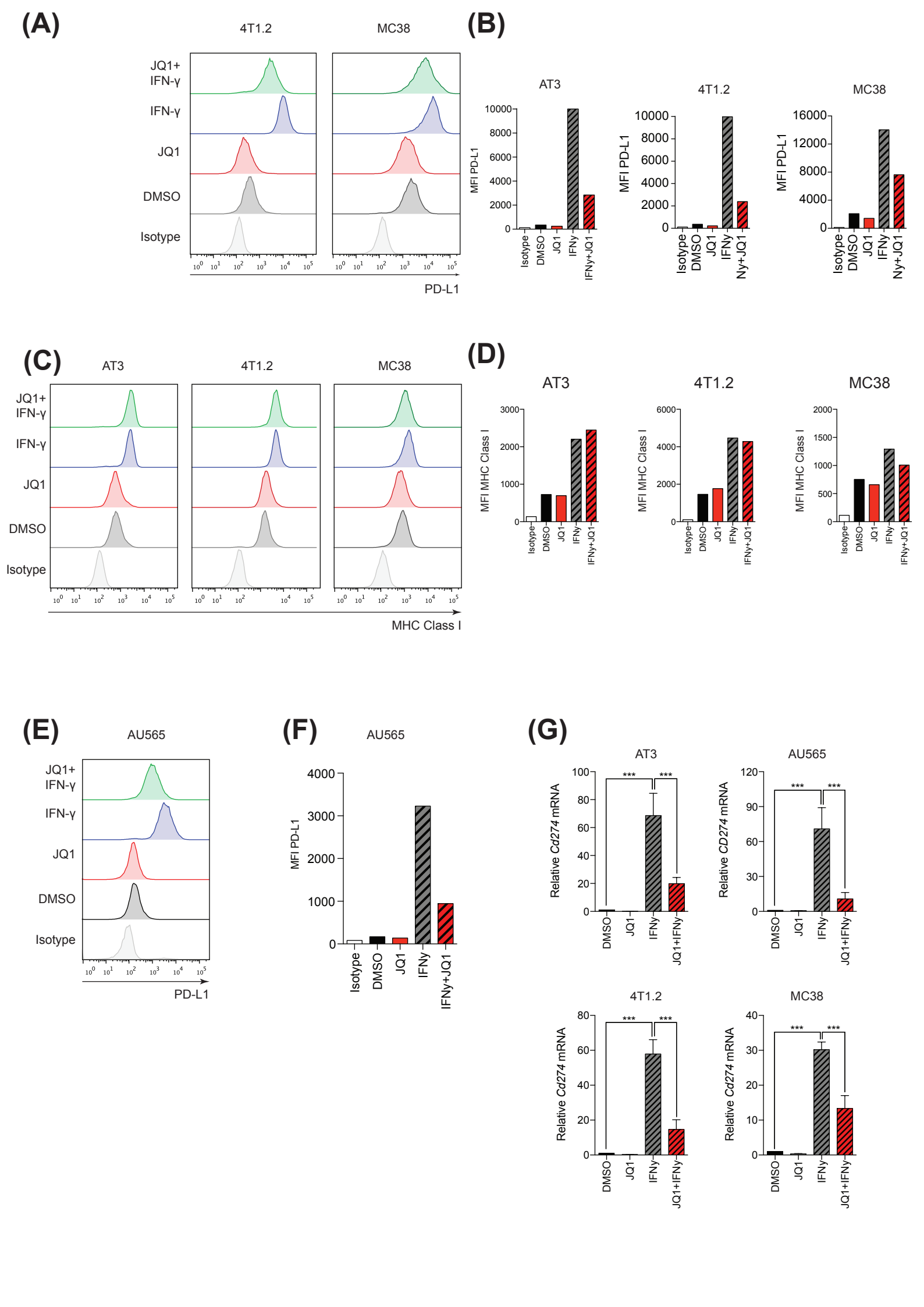
(A)
4T1.2
MC38
JQ1+ IFN-γ
IFN-γ
JQ1
DMSO
Isotype
PD-L1
(B)
AT3
4T1.2
MC38
MFI PD-L1
Isotype
DMSO
JQ1
IFNγ
IFNγ+JQ1
(C)
AT3
4T1.2
MC38
JQ1+ IFN-γ
IFN-γ
JQ1
DMSO
Isotype
MHC Class I
(D)
AT3
4T1.2
MC38
MFI MHC Class I
(E)
AU565
JQ1+ IFN-γ
IFN-γ
JQ1
DMSO
Isotype
PD-L1
(F)
AU565
MFI PD-L1
Isotype
DMSO
JQ1
IFNγ
IFNγ+JQ1
(G)
AT3
AU565
4T1.2
MC38
Relative Cd274 mRNA
DMSO
JQ1
IFNγ
JQ1+IFNγ
***

Figure S5, related to figure 6. JQ1 suppresses IFN-γ-induced PD-L1 expression in a variety of solid tumour cell lines. Mouse mammary (AT3 and 4T1.2) and mouse colon (MC38) tumour cell lines were cultured for 24 hours in the presence of 1μM JQ1, 10ng/mL mouse IFN-γ, combination of JQ1 and IFN-γ, or DMSO vehicle, prior to assessment of Pd-l1 expression by flow cytometry. Representative histograms and MFI of **(A-B)** Pd-l1 and **(C-D)** MHC Class I (H-2Kb) expression are shown for cells cultured. Human mammary (AU565) cell lines were cultured for 24 hours in the presence of 1μM JQ1, 10ng/mL human IFN-γ, combination of JQ1 and IFN-γ, or DMSO vehicle, prior to assessment of PD-L1 expression by flow cytometry. Representative histograms and MFI of **(E-F)** PD-L1 expression are shown for cells cultured. **(G)** AT3, AU565, 4T1.2, and MC38 were cultured for 2 hours in the presence of 1μM JQ1, 10ng/mL IFN-γ, combination of JQ1 and IFN-γ, or DMSO vehicle, prior to assessment of *CD274* mRNA levels by qRT-PCR. Transcript levels are normalized to *GAPDH* and presented as fold change compared to DMSO. Data presented as fold-change from 3 separate experiments ± S.E.M. (**p <0.01, ***p<0.001, Student's t test).

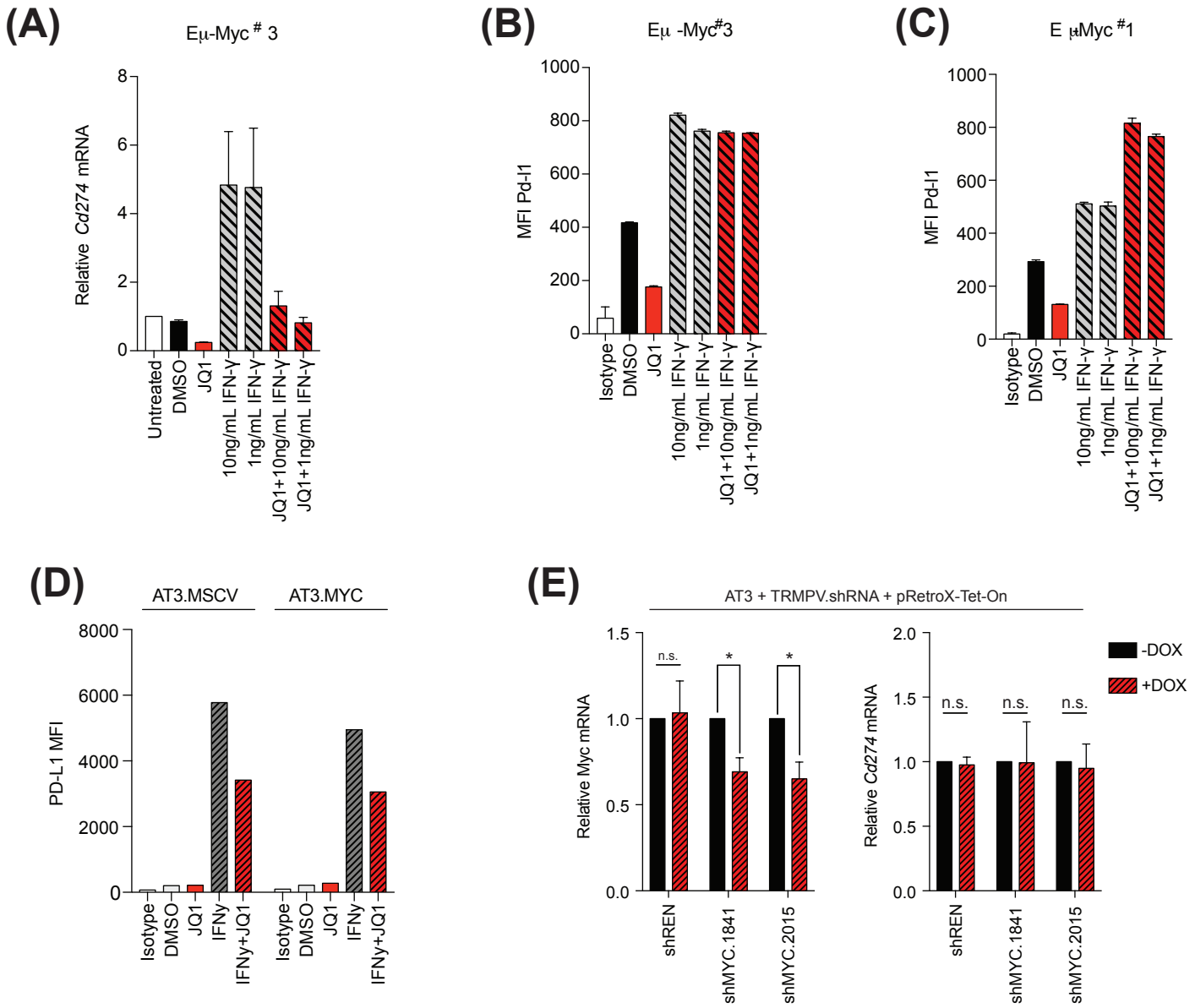
(A)
Eμ-Myc # 3
Relative Cd274 mRNA
0
2
4
6
8
Untreated
DMSO
JQ1
10ng/mL IFN-γ
1ng/mL IFN-γ
JQ1+10ng/mL IFN-γ
JQ1+1ng/mL IFN-γ
(B)
Eμ -Myc#3
MFI Pd-l1
0
200
400
600
800
1000
Isotype
DMSO
JQ1
10ng/mL IFN-γ
1ng/mL IFN-γ
JQ1+10ng/mL IFN-γ
JQ1+1ng/mL IFN-γ
(C)
E μMyc #1
MFI Pd-l1
0
200
400
600
800
1000
Isotype
DMSO
JQ1
10ng/mL IFN-γ
1ng/mL IFN-γ
JQ1+10ng/mL IFN-γ
JQ1+1ng/mL IFN-γ
(D)
AT3.MSCV
AT3.MYC
PD-L1 MFI
0
2000
4000
6000
8000
Isotype
DMSO
JQ1
IFNγ
IFNγ+JQ1
Isotype
DMSO
JQ1
IFNγ
IFNγ+JQ1
(E)
AT3 + TRMPV.shRNA + pRetroX-Tet-On
Relative Myc mRNA
0.0
0.5
1.0
1.5
n.s.
*
*
shREN
shMYC.1841
shMYC.2015
Relative Cd274 mRNA
0.0
0.5
1.0
1.5
2.0
n.s.
n.s.
n.s.
shREN
shMYC.1841
shMYC.2015
-DOX
+DOX

Figure S6, related to figure 6. JQ1 suppresses IFN-γ-induced *Cd274* transcription in Eμ-*Myc* lymphoma despite sustained protein expression; **(A)** Eμ-*Myc* #3 lymphoma cells were cultured in the presence of JQ1 (1μM), 10ng/mL or 1ng/mL recombinant mouse IFN-γ, or combinations of JQ1+IFN-γ for 2 hours prior to assessment of *Cd274* mRNA levels by qRT-PCR. Transcript levels are normalized to actin and presented as fold change compared to untreated. Data presented as fold-change from 3 separate experiments ± S.E.M. **(B)** Eμ-*Myc* #3 lymphoma cells were cultured in the presence of JQ1 (1μM), 10ng/mL or 1ng/mL recombinant mouse IFN-γ, or combinations of JQ1+IFN-γ for 24 hours prior to assessment of cell surface Pd-l1 expression by flow cytometry. **(C)** Eμ-*Myc* #1 lymphoma cells were cultured in the presence of JQ1 (1μM), 10ng/mL or 1ng/mL recombinant mouse IFN-γ, or combinations of JQ1+IFN-γ for 24 hours prior to assessment of cell surface Pd-l1 expression by flow cytometry.Overexpression or genetic depletion of Myc does not modulate IFN-γ-induced or basal Pd-l1 expressionl; **(D)** AT3 cells transduced with MSCV.GFP or MSCV.hsMYC.GFP were cultured for 24 hours in the presence of 1μM JQ1, 1ng/mL IFN-γ, combination of JQ1 and IFN-γ, or DMSO vehicle, prior to assessment of Pd-l1 expression by flow cytometry. Representative data is presented as MFI of cells cultured. **(E)** *Myc* and *Cd274* mRNA levels were determined by qRT-PCR in AT3 cells were transduced with tetracycline-inducible shRNAs targeting Myc (#1891 and #2105) or Renilla (REN) and exposed to doxycycline for 18 hours. Transcript levels are normalized to Actin and presented as fold change compared to -DOX. Data presented as fold-change from 3 separate experiments ± S.E.M. (*$p < 0.05$, Student's t test).

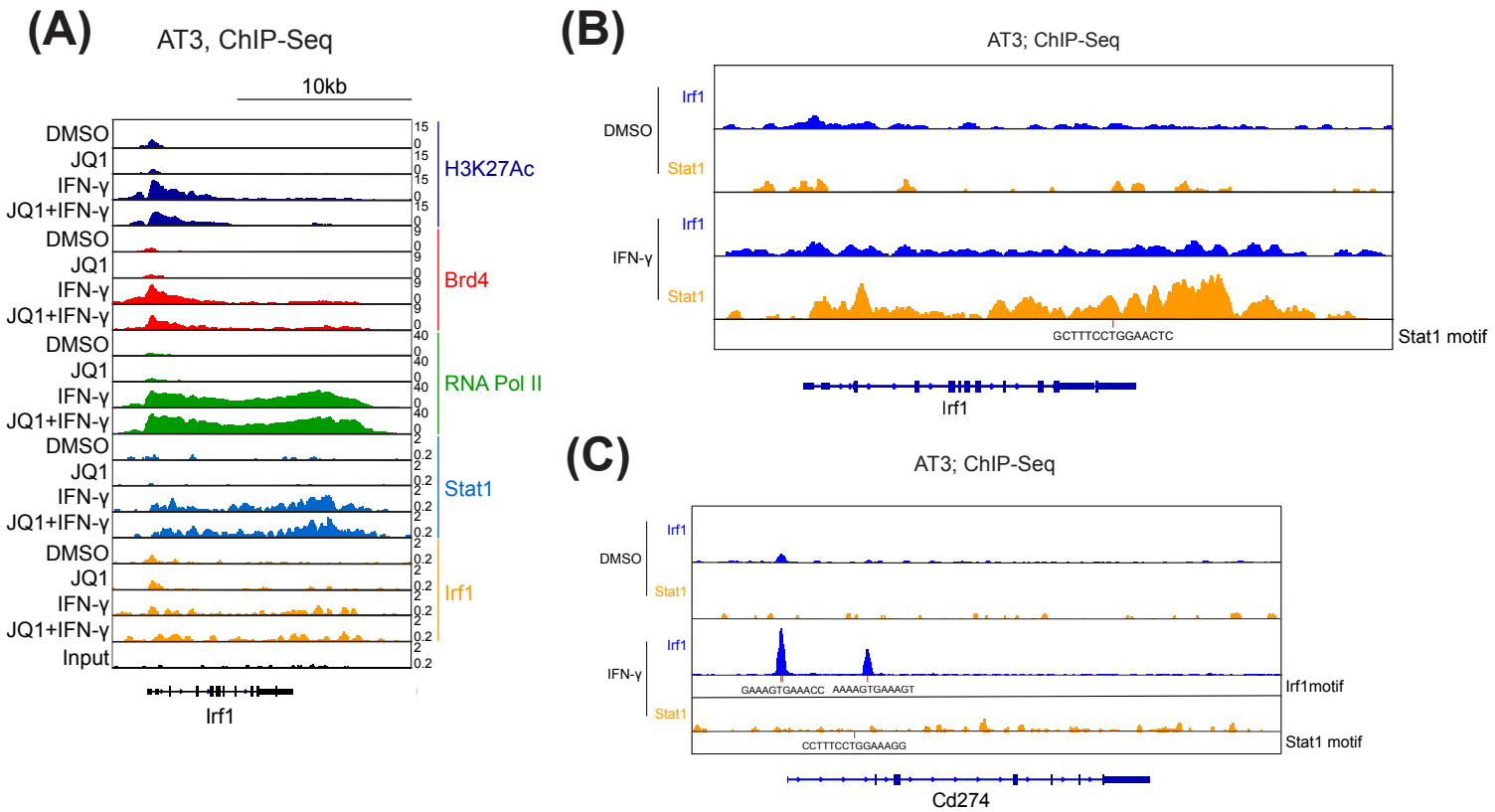
(A)
AT3, ChIP-Seq
10kb
DMSO
JQ1
IFN-γ
JQ1+IFN-γ
H3K27Ac
Brd4
RNA Pol II
Stat1
Irf1
Input
Irf1
(B)
AT3; ChIP-Seq
Irf1
Stat1
GCTTTCCTGGAACTC
Stat1 motif
Irf1
(C)
AT3; ChIP-Seq
GAAAGTGAAACC
AAAAGTGAAAGT
Irf1motif
CCTTTCCTGGAAAGG
Stat1 motif
Cd274
(D)
Eμ-Myc #1
#1/PD-L1
#1/MSCV
Isotype
% of maximum
PD-L1 [PE]

Figure S7, related to figure 5. Stat1 is recruited to the Irf1 locus following IFN-γ stimulation; **(A)** Visualization of H3K27Ac, Brd4, RNA Pol II, Irf1, and Stat1 occupancy at the *Irf1* locus in AT3 cells cultured for 2 hours in the presence of 1μM JQ1, 1ng/mL IFN-γ, combination of JQ1 and IFN-γ, or DMSO vehicle, prior to ChIP-Seq analysis. **(B)** Visualization of Irf1 and Stat1 recruitment to the *Irf1* locus following IFN-γ stimulation for 2 hours, with Stat1 and Irf1 consensus binding motifs indicated. No Irf1 motifs were identified at this locus. **(C)** Visualization of Irf1 and Stat1 recruitment to the *Cd274* locus following IFN-γ stimulation for 2 hours, with Stat1 and Irf1 consensus binding motifs indicated. Ectopic expression of murine Pd-l1 from a retroviral promoter; **(D)** Eμ-*Myc* lymphoma #1 cells were retrovirally transduced with murine stem cell virus (MSCV-BFP) containing murine Pd-l1 cDNA (#1/PD-L1) or empty vector control (#1/MSCV). BFP^+ cells were isolated by FACS sorting and Pd-l1 expression was assessed by flow cytometry.